

Memory effect and spin-glass-like behavior in Co-Ag granular films

J. Du,^{1,2} B. Zhang,¹ R. K. Zheng,¹ and X. X. Zhang^{1,*}

¹*Department of Physics and Chemistry and Institute of Nano Science and Technology,*

The Hong Kong University of Science and Technology, Clear Water Bay, Kowloon, Hong Kong

²*National Laboratory of Solid State Microstructures and Department of Physics, Nanjing University, Nanjing 210093, People's Republic of China*

(Received 9 May 2006; revised manuscript received 9 November 2006; published 11 January 2007)

The memory effect was clearly observed in dc-sputtered metallic, magnetic Co-Ag granular films, which indicates the existence of a spin-glass-like phase at low temperatures. However, the memory effect diminished dramatically after the films were annealed at 300 °C for 1 h. It was also found that the memory effect weakened gradually with increasing volume fraction of magnetic clusters. The experimental results indicate that the dipolar interaction is not the major origin for the formation of low-temperature spin-glass-like (SGL) phase in metallic, magnetic granular materials. On the other hand, a Ruderman-Kittel-Kasuya-Yosida-like exchange interaction between the nanoparticles may be responsible for the collective SGL dynamics and the resulting memory effect.

DOI: [10.1103/PhysRevB.75.014415](https://doi.org/10.1103/PhysRevB.75.014415)

PACS number(s): 75.50.Lk, 75.10.Nr, 75.75.+a

INTRODUCTION

The low-temperature dynamics of interacting magnetic nanoparticles has been a subject of growing interest in the study of magnetism for several decades.¹⁻¹² An assembly of magnetic nanoparticles is, in general, a disordered system with random anisotropy and competing interparticle interactions.¹² In a very diluted system, i.e., where interparticle dipole-dipole interactions are negligibly small in comparison with anisotropy energy, the dynamics of particles are well described by the superparamagnetism framework of the Néel-Brown model.^{13,14} That is, the flipping rate (Γ) of the magnetic moment of an individual magnetic particle is only governed by its own anisotropy energy at a given temperature (T), $\Gamma(T) = \Gamma_0 \exp(-KV/k_B T)$, where Γ_0 is the attempt frequency in the order of $10^9 - 10^{13}$; k_B is the Boltzmann constant; K and V are the anisotropy constant and the volume of particle respectively.¹⁵ $\Gamma(T)$ decreases exponentially with decreasing temperature. When $KV \gg k_B T$, the magnetic moment is frozen in one direction of its easy axis, that is, the flipping is blocked. At high temperatures, the moment flipping between two directions of its easy axis is well described by superparamagnetism.

As the particle concentration increases (the interparticle distance decreases), dipole-dipole interactions will certainly affect the dynamics of magnetic moment. For not very strongly interacting particles, the dynamics of each magnetic moment can still be considered individually, i.e., superparamagnetism, but with a modified energy barrier. For example, based on the calculation of interaction energies of a particle with each of its neighbors, Dormann *et al.* pointed out that the effect of dipole-dipole interaction can be considered as an extra energy barrier adding to its anisotropy energy,¹⁶ i.e., $\Gamma(T) = \Gamma_0 \exp[-(KV + E_{\text{int}})/k_B T]$, where E_{int} is the interaction energy. This model predicted that the flipping of magnetic moment slows down with increasing dipole-dipole interaction. The superparamagnetic model with modified energy barrier was quite successful in interpreting experimental observations for different interacting particle systems¹⁷⁻¹⁹ and

has been recently confirmed by Monte Carlo simulations.²⁰

Interestingly, Mørup and Tronc²¹ proposed a different form of effective energy barrier for the superparamagnetic model and successfully explained their experimental results obtained on weakly interacting $\gamma\text{-Fe}_2\text{O}_3$ particles. The effective barrier, proposed by Mørup and Tronc, decreases with increasing dipole-dipole interaction, which consequently predicts an enhanced flipping of magnetic moment by dipole-dipole interaction.

Contrary to the superparamagnetic model, cooperative freezing, or spin-glass-like (SGL) phase was proposed to account for low-temperature phenomena observed experimentally in different interacting-particle systems. The existence of a low-temperature spin-glass phase in the magnetic nanoparticle systems has been evidenced by the observation of different effects, such as aging and memory effects,^{1,3,7,8,10,11} critical slowing down of relaxation rate,^{1,3,7,8} critical behavior at finite temperature,^{3,4} and flat field-cooling (FC) curves below freezing temperature.⁵ Monte Carlo simulation results also show that magnetic aging and a drastically broadened relaxation function appear at low temperature when the interactions become strong enough, which suggests that the collective nature of the dynamics of particles is important.⁸

However, one may observe the SGL behavior in noninteracting nanoparticles, due to core-shell structures of nanoparticles. For example, oxide particles may have a SGL shell as observed in NiFe_2O_4 (Ref. 22) and $\gamma\text{-Fe}_2\text{O}_3$ (Ref. 23) nanoparticles. To our best knowledge, the SGL phase has been mainly observed in some special particle systems, such as the magnetic frozen fluid composed of $\gamma\text{-Fe}_2\text{O}_3$, $\varepsilon\text{-Fe}_3\text{N}$, and $\text{Fe}_x\text{C}_{1-x}$ particles,^{3-5,7} and a discontinuous $[\text{Co}_{80}\text{Fe}_{20}(0.9 \text{ nm})/\text{Al}_2\text{O}_3(3 \text{ nm})]_{10}$ multilayer.²⁴ In these samples, there is probably a surface layer on the particles that does not have the same magnetic state as the particle core and may exhibit SGL behavior.^{22,23} Therefore, one may ask what is the origin of spin-glass-like phenomenon in low-temperature interacting nanoparticle systems.

In this work, metallic Co-Ag granular films were studied so as to answer this question. The advantages of using me-

tallic granular systems are that (a) there is a no-oxide layer surrounding the magnetic clusters and (b) the sample is stable and can be used repeatedly. Most studies on how dipole-dipole interactions lead to SGL phase in particles systems were carried out by changing the concentration of particles (particle-particle distance) in the liquid carrier.^{1–11,14} Here, we studied the same issue by changing the particle (or cluster) size and the concentration of solute Co atoms in Ag matrix. We focused on the study of memory effect because it is usually considered as typical characteristics of the spin-glass dynamics and has been clearly observed in different (canonical) spin-glass systems.^{25–27} Although the spin-glass state was found in Fe-Cu (Ref. 28) and Co-Cu (Ref. 29) granular films, and the memory effect in FeCo-Al₂O₃ discontinuous multilayers,²⁴ we report on the memory effect in metallic, magnetic granular films.

The memory effect was clearly observed in all sputtered Co_xAg_{1-x} granular films with Co volume fractions of 9.6% $\leq x \leq 19.4\%$, which indicates the existence of a spin-glass-like or cooperative freezing phase. The most interesting observation is that the memory effect dramatically weakened after the samples were annealed at 300 °C for 1 h.

EXPERIMENTAL

Co-Ag granular films were fabricated by cosputtering technique on glass or Kapton substrate at room temperature. The base pressure was below 2×10^{-7} Torr and the Ar pressure was 4×10^{-3} Torr during deposition. Films of different compositions were deposited by adjusting the sputtering power of Co and Ag targets. The film thickness was kept at about 0.45 μm for all the samples. The atomic concentrations of the films were obtained using x-ray fluorescence (XRF) technique, and the volume fraction, x , was then calculated. In this paper, three representative samples with Co volume fractions of 9.6% (S1), 12.7% (S2), and 19.4% (S3) are discussed. The corresponding Co atomic ratios are 14.1%, 18.4%, and 27.2%, respectively. To investigate the effect of annealing, films were cut into several pieces. The as-sputtered films were then annealed under vacuum with pressure lower than 1×10^{-6} Torr for 1 h at different temperatures. The structures of the films were characterized using both x-ray diffraction (XRD) and transmission electron microscopy (TEM). The magnetic properties of the films were measured by a commercial Quantum Design superconducting quantum interference device (SQUID) magnetometer. The magnetoresistance was measured by a standard four-probe method using a commercial Quantum Design physical measurement system (PPMS-9).

RESULTS AND DISCUSSION

Figure 1 shows the XRD patterns of a representative sample, i.e., sample S1, in the as-deposited and annealed states at 300 °C and 400 °C, respectively. Only the face-centered-cubic (fcc) Ag (111) and (222) peaks can be clearly observed in the as-deposited state. However, there exists a “shoulder” around the position of fcc Co (111) peak, indicating that very small Co particles or clusters were embedded in

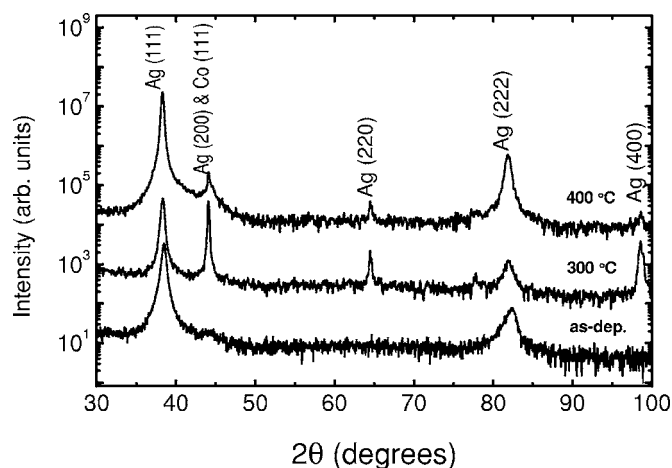
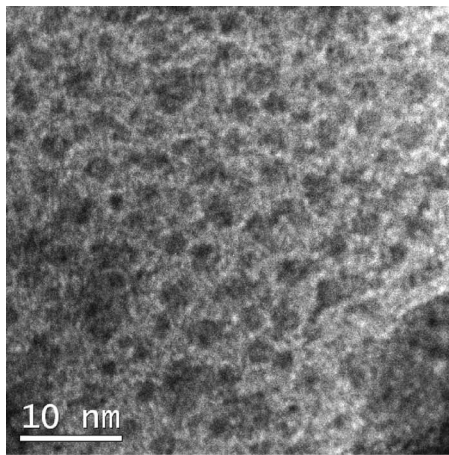


FIG. 1. X-ray diffraction patterns of the S1 samples of as-deposited, annealed at 300 °C and 400 °C for 1 h, respectively.

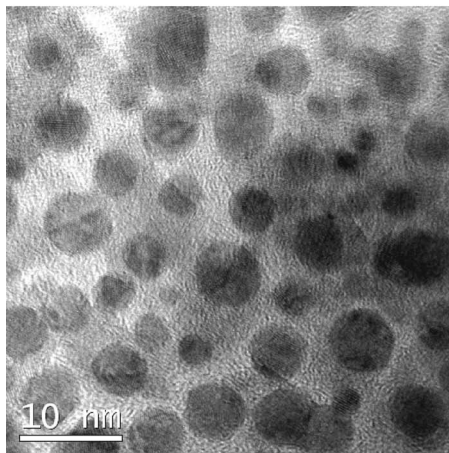
the Ag matrix. The other two samples, S2 and S3, had similar XRD patterns. After annealing, the fcc Co (111) diffraction peak obviously emerges, indicating the formation and precipitation of fcc Co-rich particles from the Ag-rich matrix, which is in agreement with the observation by De Toro *et al.*³⁰ The corresponding change in the morphology and structure of the S1 sample before and after annealing has also been verified by TEM imaging as shown in Fig. 2. In the as-deposited sample, Co-rich particles cannot be clearly seen due to the formation of very small clusters and the metastable alloying with Ag. However, after annealing at 300 °C, much larger Co-rich particles are clearly seen in the TEM images, indicating that Co and Ag are well separated. The texture and microstructure of these Co-rich particles can also be verified by high-resolution TEM (HRTEM) and selected area diffraction (SAD) (not shown here). The Co-rich particles are approximately spherical with a size distribution from 2 to 5 nm. These microscopic features are very similar to those described in previous studies.³¹

Although the mutual solubility equilibrium of Ag and Co is very low, a much larger concentration of solute Co atoms should be expected in Co-Ag films deposited by the nonequilibrium sputtering technique at room temperature. Since the concentration of solute Co atoms in the matrix plays an important role in determining the interactions within the granular films,^{30,32} we extracted the concentration of solute Co atoms in the as-deposited and annealed films. The concentration of solute Co atoms can be easily calculated from the shift in the Bragg diffraction peaks of Ag (111) or (222) from the bulk solutions if we assume the alloying of Co and Ag follows Vegard’s law.³³ The calculated values are 6.9%, 3.5%, and 3.0% for as-deposited and annealed at 300 °C and 400 °C, respectively, of the S1 samples. These results show unambiguously that in the as-deposited Co-Ag film, a fairly large amount of cobalt atoms dissolve in the silver matrix and that the concentration of solute Co atoms is dramatically reduced after annealing at a temperature higher than 300 °C due to remarkable segregation of cobalt from the matrix.^{30,32}

The above arguments may also be supported by the giant magnetoresistance (GMR) data. Magnetoresistance (MR) measurements were carried out under a magnetic field of



(a)

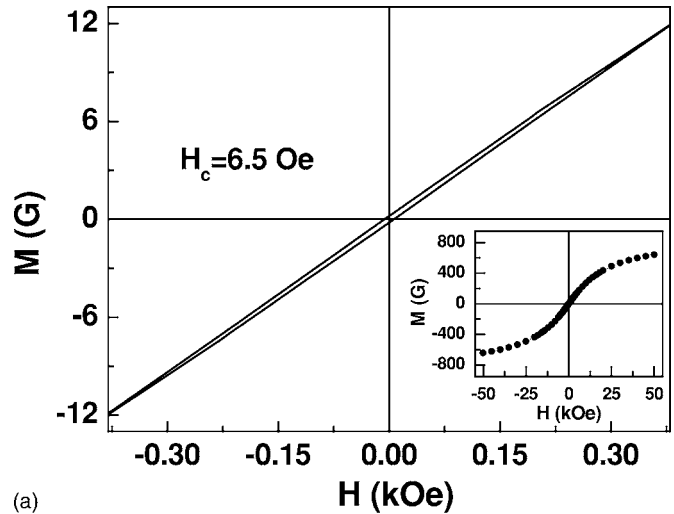


(b)

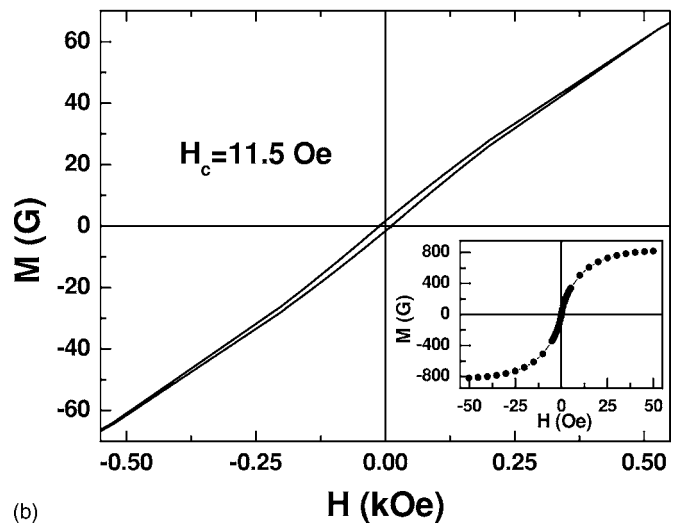
FIG. 2. TEM images of the S1 sample, (a) as-deposited and (b) annealed at 300 °C for 1 h.

5 T. For sample S1, the GMR decreased monotonically from 21.0% to 5.0% when temperature increased from 5 K to 300 K; after it was annealed at 300 °C, the GMR dropped from 24.3% to 7.8% as temperature increased from 5 to 300 K, i.e., the MR was enhanced in the whole temperature range. The enhanced MR, in spite of the reduction of interface density due to particle coalescence (see Fig. 2), indicates that the indirect exchange interactions mediated by solute Co atoms weakened as the Co concentration decreased in Ag matrix.³⁰

We also measured the field-dependent magnetization, M - H , loops for all samples before and after annealing within a temperature range of 5 to 300 K. As was discussed by Alia *et al.*, dipole-dipole interaction between the clusters can be evidenced by a thin, elongated hysteresis loop measured at a temperature much higher than blocking temperature.³⁴ And noninteracting clusters must show a reversible magnetization curve at a temperature much higher than their blocking temperatures, i.e., the coercive field is zero. The thin, elongated hysteresis loops have been clearly observed for all our samples. Shown in Figs. 3(a) and 3(b) are the 300 K hysteresis loops in the vicinity of zero field for sample S1 before and after annealing at 300 °C. The insets of the Fig. 3



(a)



(b)

FIG. 3. M - H loops of S1 sample measured at $T=300$ K in the vicinity of zero field, (a) as-deposited and (b) annealed at 300 °C. Insets are the corresponding hysteresis loops in the field range of -50 kOe to 50 kOe.

are the corresponding hysteresis loops in the field range of -50 to 50 kOe. The thin, elongated loops in Fig. 3 clearly indicate the existence of dipole-dipole interaction in both samples. Most interestingly, the coercive field in the annealed sample, $H_c=11.5$ Oe, is much larger than $H_c=6.5$ Oe in the as-deposited film, which strongly suggests that the dipole-dipole interaction was significantly enhanced after annealing. The enhanced dipole-dipole interaction can be understood through the simple model described later.

Figure 4 shows the temperature-dependent magnetization measured in the zero-field-cooled (ZFC) and field-cooled (FC) processes with a 20 Oe field on the S1 samples (as-deposited and annealed at 300 °C), S2 and S3 samples. The peak temperatures of the ZFC curves are 30 K, 43.5 K, and 83 K for S1, S2, and S3, respectively. For the as-deposited samples, the ZFC and FC curves separate at a temperature (bifurcation temperature), which is very close to the peak temperature of ZFC curves, suggesting a collective spin-glass-like behavior below T_p .³⁵ The existence of a coopera-

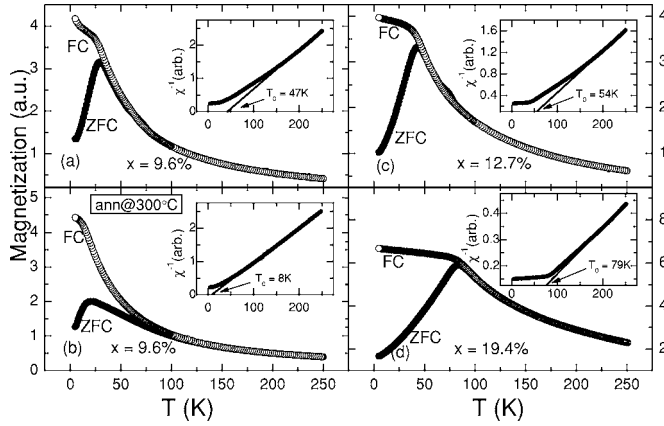


FIG. 4. ZFC-FC magnetization versus temperature curves for (a) S1 as-deposited, (b) S1 annealed at 300 °C, (c) S2, and (d) S3. The insets show the inverse susceptibility versus temperature for all the samples, respectively.

tive spin-glass phase has been confirmed by the observation of memory effect, an inherent characteristic of a spin-glass behavior. The increasing ZFC peak temperature (with increasing Co concentration) indicates, first of all, a higher intensity in interparticle interactions, since the ZFC maximum signals a “superspin glass” temperature determined by those interactions. These increasing interactions, in turn, are due to larger size and concentration of Co particles.

Figure 4(b) shows the ZFC and FC curves of annealed S1 at 300 °C for 1 h. Two major changes can be clearly seen in this ZFC-FC curve in comparison with that shown in Fig. 4(a). First, the bifurcation temperature between ZFC and FC curves increases significantly. It is well known that the bifurcation temperature can be considered as the blocking temperature of the largest particles for a system composed of weakly interacting particles with a size distribution.¹⁵ Therefore, this increase can be attributed to the growth of Co-rich particles after they precipitate from the Ag-rich matrix. On the other hand, T_p decreases from 30 K to 22 K, which can be ascribed to the reduction of indirect exchange interaction [the Ruderman-Kittel-Kasuya-Yosida (RKKY) interaction]³⁰ as a consequence of decreasing concentration of the solute Co atoms in Ag matrix. When the sample was annealed at 400 °C (not shown here), the bifurcation temperature and T_p were both higher than 300 K, indicating that most of the Co clusters are large enough to be stable (in a blocked state) at room temperature.

In order to explore the effective interactions in Co-Ag granular system, we plot χ^{-1} ($=H/M$) in relation to the temperature of FC curve, as shown in the insets of Fig. 4. It is well known that in the superparamagnetic regime ($T > T_B$, where T_B denotes the blocking temperature), the magnetic susceptibility of a nanoparticle system can be described by Curie-Weiss law,³⁶

$$\chi = \frac{M}{H} = \frac{xVM_S^2(T)}{3k_B(T - T_0)} \text{ for } \mu H < k_B T, \quad (1)$$

where x is the volume fraction of magnetic particles, V is the particle volume, $M_S(T)$ is the spontaneous magnetization, k_B

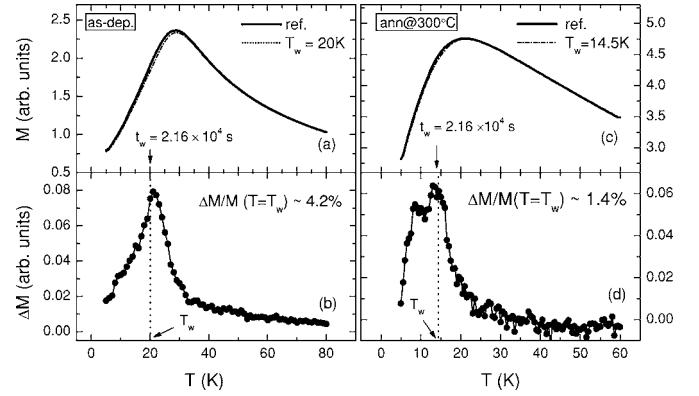


FIG. 5. (a) and (c) show the ZFC magnetization versus temperature for S1 as-deposited and S1 annealed, respectively. The solid lines indicate the reference curves and the dotted lines indicate the stop-and-wait curves. (b) and (d) show the excess magnetization (ΔM) versus temperature for S1 as deposited and S1 annealed, respectively.

is the Boltzmann constant, and μ ($=M_S V$) is the magnetic moment of a single particle with volume V . The absolute value of T_0 reflects the strength of interaction.

By extrapolating χ^{-1} from linear part of the high-temperature region to $\chi^{-1} \sim 0$, we obtained $T_0 = 47$ K, 54 K, and 79 K for samples S1, S2, and S3 respectively, indicating that the strength of effective interaction among clusters increases monotonically with increasing Co volume fraction. The positive T_0 's indicate that ferromagneticlike interactions are dominant. Interestingly, T_0 decreases dramatically from 47 K to 8 K for the S1 sample after annealing, suggesting that the effective interaction weakens dramatically.

As described in the introduction, SGL behaviors, such as the memory effect, can be observed when the dipolar interactions between magnetic nanoparticles are strong enough. In a typical dc memory experiment, one should follow a stop-and-wait protocol consisting of three steps:^{14,24} (a) cool the sample in a zero-field at a constant rate from a temperature, T_H , which is much higher than T_p , the peak temperature of ZFC curves; (b) stop the cooling process at a temperature, T_w , below T_p and wait for t_w ($=6$ h, in our experiments) and then resume the cooling process down to T_{base} ($=5$ K in our experiments); (c) apply a small field at T_{base} and measure the magnetization with increasing temperature up to T_H . The difference between the stop-and-wait ZFC curve and a reference ZFC curve (without stopping at T_w) at the temperature T_w can be attributed to the memory effect.

Figures 5(a) and 5(c) show the reference and stop-and-wait ZFC dc magnetization curves for the S1 sample in the as-deposited and annealed states. The overlapping region of the two curves covers almost the entire measuring temperature range except in the vicinity of T_w . In order to clearly show the difference between two curves, we plot the difference in magnetization, $\Delta M(T) [=M_{\text{ref}}(T) - M(T)]$ in Figs. 5(b) and 5(d). The maximum in $\Delta M(T)$ appears *exactly* at T_w , which is the signature of memory effect. Similar memory effects were also observed for S2 and S3 samples with relatively higher Co volume fractions (not shown here).

The memory effect observed in our samples can certainly be understood through hierarchical model^{27,37,38} and droplet

model.^{17,37–40} Both models are quite successful in describing the memory effect in spin-glass systems.²⁷ We will not reiterate them here.

To compare the relative strength of the memory effect, we introduce a parameter, i.e., the ratio of $\Delta M/M$ at the waiting temperature (T_w). We observed that ΔM depends strongly on the waiting time because of the logarithmic relaxation.^{14,41} In addition, it also varies with T_w . To reduce the complexity caused by the waiting time and T_w , we fix the waiting time to be 2.16×10^4 seconds (i.e., 6 h) and the ratio of T_w/T_p (or T_w/T_F) to be about 0.7, where the magnetic relaxation is neither too slow nor too fast to observe the memory effect. Therefore, the $\Delta M/M$ ($T=T_w$) ratio can reflect the strength of memory effect nearly quantitatively. Due to different peak temperatures of the samples, T_w has been chosen to be 20 K, 14.5 K, 29 K, and 57 K for S1 as-deposited, S1 annealed, S2, and S3 samples, respectively. The calculated values of $\Delta M/M$ are 4.2%, 1.4%, 3.8%, and 2.8%, respectively. It is obvious that the value of $\Delta M/M$ decreases, i.e., the memory effect weakens significantly after annealing. Another surprising observation is that by increasing the Co content, the effective interaction enhances significantly (indicated by increasing the value of T_0), while the memory effect weakens gradually.

What is the major origin or dominant interaction leading to the SGL collective dynamics or memory effect? It is well known that, in granular systems with metallic matrices, despite the diverse and complicated correlative interactions, two types of important interactions should be considered at the very beginning: the dipolar and RKKY-like interactions.

The energy of interparticle dipole-dipole interactions can be described as²⁰

$$E_D^{(i,j)} = \frac{\mu_0}{4\pi} \left[\frac{\vec{\mu}_i \cdot \vec{\mu}_j}{r_{ij}^3} - \frac{3(\vec{\mu}_i \cdot \vec{r}_{ij})(\vec{\mu}_j \cdot \vec{r}_{ij})}{r_{ij}^5} \right] \quad (2)$$

where r_{ij} is the distance between localized magnetic moments, $\vec{\mu}_i$ and $\vec{\mu}_j$, on different particles (clusters). The absolute value of magnetic moment $\vec{\mu}_i$ can be expressed as $|\vec{\mu}_i| = M_S V$, where M_S is the saturation magnetization of a particle and V is its volume.

In order to simplify the calculation and understand the key feature of dipolar interaction energy in a granular system, we make the following approximations: (1) the volume fraction, ε , remains constant before and after annealing, due to the fact that the annealing temperature in our experiments is much lower than the evaporating temperature of Co and Ag; (2) Co clusters are spherical with uniform size (R) and homogeneous distribution; and (3) Co clusters form a simple cubic lattice with a lattice constant, A . Therefore, ε can be simplified as

$$\varepsilon = \frac{4\pi}{3} \left(\frac{R}{A} \right)^3, \quad (3)$$

where R is the radius of the cluster. Since the values of first and second terms in Eq. (2) are both proportional to μ^2/r^3 , the order of dipolar interaction energy can be evaluated as

$$\frac{E_D}{k_B} \propto \frac{\mu_0}{4\pi k_B A^3} \frac{\mu^2}{A^3} = \frac{\mu_0}{4\pi k_B} \frac{\left(M_S \frac{4\pi}{3} R^3 \right)^2}{A^3} = \frac{4\pi \mu_0 M_S^2}{9 k_B} \left(\frac{R}{A} \right)^3 R^3. \quad (4)$$

Therefore, by substituting Eq. (2) in Eq. (4), Eq. (4) can be written as³²

$$\frac{E_D}{k_B} \propto \frac{\mu_0}{4\pi k_B} M_S^2 V \varepsilon. \quad (5)$$

Here, $V=(4\pi/3)R^3$. It is well known that the diameter of clusters in the annealed sample (R_2) is usually larger than that in the as-prepared samples (R_1), i.e., $R_2 > R_1$, which is confirmed by the TEM image shown in Fig. 2. Then,

$$\frac{E_D^1}{E_D^2} = \left(\frac{R_1}{R_2} \right)^3 \ll 1.$$

Therefore, we expect a much stronger dipole-dipole interaction in the annealed samples. One may argue that the model may be too simplified and may neglect some other factors which influence the dipolar interaction. For example, after annealing, the shape of the magnetic clusters may change to a ‘‘pancake’’ shape with the short axis along the film’s normal.⁴² The dipolar interaction may not be enhanced as fast as $(R_2/R_1)^3$. However, according to the above simple analysis, it is reasonable to believe that the dipole-dipole interaction between magnetic clusters should be enhanced after annealing. The enhanced dipole-dipole interaction was indeed observed from room temperature hysteresis loops shown in Fig. 3.

If the dipolar interactions play a major role leading to memory effect (or the SGL phase) in Co-Ag granular films, a much more pronounced memory effect should be observed in the annealed samples. This is *absolutely* contradictory to our observations, suggesting that the dipole-dipole interaction is very unlikely to be the dominant interaction leading to the formation of spin-glass-like phase in these Co-Ag granular films. Therefore, we wonder which interaction is the dominant one in Co-Ag films.

Since the Co-Ag granular films is a nonequilibrium, metallic magnetic system, RKKY-like interactions should be expected to exist and strongly enhanced by the presence of magnetic solute atoms, which has been demonstrated previously in different metallic, magnetic granular systems.^{30,32} However, after annealing, the solute cobalt atoms precipitate from the matrix and the Co-rich particles grow as well. This will have a dramatic effect on the effectiveness of RKKY-like interactions due to Co depletion of the shell surrounding each Co particle.^{30,32} As a result, the RKKY-like interparticle interactions become too weak to lead to a collective magnetic behavior (SGL phase). It should be noted that RKKY-like interactions were also invoked to explain the superspin glass transition in other nanogranular materials.⁴³

The above arguments seem to be plausible in accounting for the influence of annealing on the memory effect in our samples. According to above analysis, the concentration of solute Co atoms in Ag matrix seems to be an important factor

mediating the strength of RKKY-like interaction. For S1 sample in the as-deposited state, as we mentioned previously, the concentration of solute Co atoms in Ag is about 6.9% (nearly half of the total amount) that dissolved in the Ag matrix to form a metastable Co-Ag alloy. The rest of cobalt atoms should form nanometer-scale Co-rich particles or clusters embedded in the Co-Ag alloy. Therefore, RKKY-like interactions among Co particles are enhanced through solute Co atoms, which leads to a pronounced memory effect. However, after annealing at 300 °C, due to precipitation, the concentration of solute Co atoms in Ag matrix changed to 3.5%. At the same time, the nanoparticles grew larger due to aggregation or coarsening,³⁰ which was confirmed by the higher bifurcation temperature in Fig. 4(b). This process will undoubtedly reduce RKKY-like interactions significantly and the SGL phase will not likely be maintained any longer. In our case, the system seems to be a mixture of spin-glass-like and superparamagnetic phases because of the fact that memory effect does not diminish to zero.

The reduction of T_p from 30 K to 22 K after annealing at 300 °C can also be attributed to the inhibition of RKKY-like interactions.³⁰ The reduction of T_p is consistent with the results reported by De Toro *et al.*³⁰ in $\text{Co}_{29}\text{Ag}_{71}$ and $\text{Co}_{25}\text{Ag}_{75}$ (atomic fractions) granular films with almost the same annealing temperature (298 °C). However, as we mentioned previously, if the annealing temperature increases up to 400 °C, the ZFC and FC curves (not shown here) will no longer coalesce within the measuring temperature range. The T_p of ZFC curve will also exceed the room temperature, indicating that the Co-rich particles are large enough to be at the blocked state at room temperature. Although the concentration of solute Co is still about 3%, the interparticle RKKY-like interactions should reduce further due to the increase of Co depletion shell surrounding Co particles. On the other hand, the dipolar interaction is not strong enough to lead to a collective SGL behavior, although it does increase. This has been demonstrated by the nearly undetectable memory effect in the annealed samples.

Finally, we discuss the influence of Co concentration on the memory effect. As we mentioned before, in the as-deposited samples, the memory effect weakens gradually with increasing volume fraction of Co from 9.6% to 19.4% (i.e., atomic ratio of 14.1% to 27.2%). Based on the XRD patterns of S2 and S3 samples (not shown here), we found that the concentration of solute Co atoms is about 8% in both cases, which is slightly larger than that in the S1 sample (6.9%). This means the enhancement of RKKY interaction in S2 and S3 arising from dissolved Co atoms should be comparable or slightly stronger than that in S1. On the other hand, the mean size of Co-rich particles should increase with increasing Co concentration, which can be clearly seen by the significant increase in the peak temperatures of ZFC curves in Figs. 4(a), 4(c), and 4(d). Consequently, according to Eq. (4), the dipolar interaction should increase dramatically.

The fact that the value of T_0 increases monotonically with increasing Co concentration also reflects the strengthening of effective interaction. We point out that the dipolar interaction plays a dominant role in granular films when the Co concentration is above a critical concentration as theoretically predicted.⁴⁴ However, the positive T_0 's indicate that ferromagneticlike interactions are dominant, which favors the superferromagnetic phase rather than spin-glass phase, as observed by De Toro *et al.*³⁰

Based on the magnetic phase diagram of a granular system with an insulating matrix proposed by Petravic *et al.*,⁴⁵ at sufficiently high concentrations, granular systems with dipolar interactions do not exhibit a superspin glass transition, but a “superferromagnetic transition.” It is natural to believe that in the metallic, magnetic granular systems, at a high enough concentration, ferromagneticlike interactions dominate over antiferromagneticlike ones, and thus the condition of competing interactions leading to spin-glass behavior is not fulfilled. This will certainly weaken the memory effect when the concentration of magnetic entities exceeds a certain value. Actually, in order to verify these arguments, we have fabricated Co-SiO₂ granular films. Since the RKKY-like interaction is absent in these nonmetallic systems, the dipolar interaction should play a dominant role in the films with concentrations below the percolation threshold. We found that when Co volume fraction increases, the strength of memory effect changes nonmonotonically, i.e., it increases very slowly with increasing Co concentration from zero and then decreases dramatically after the Co volume fraction exceeds 45%. Detailed results will be published elsewhere.⁴⁶

SUMMARY

We have studied the memory effect in metallic, magnetic granular films prepared using a cosputtering method. The memory effect was clearly observed in the as-deposited samples, indicating the existence of spin-glass-like phase at low temperatures. The memory effect was significantly weakened in the annealed samples in which the dipolar interaction should be significantly enhanced. In addition, with increasing magnetic metal volume fraction, the memory effect weakens gradually. A simple model suggests that the dipolar interaction does not play a key role in the formation of spin-glass-like phase in these metallic Co-Ag granular films. The observed memory effect may be ascribed to the RKKY-like interactions mediated by solute Co atoms in the Ag matrix.

ACKNOWLEDGMENTS

This work was supported by the Hong Kong RGC Grants (No. 605704 and No. 605605). One of the authors, J.D., would also like to thank the National Science Foundation of China (Grant No. 10474038) and the State Key Project of Fundamental Research Grants (No. 001CB610602) of China for partial support.

- *Corresponding author. Electronic address: phxxz@ust.hk
- ¹T. Jonsson, J. Mattsson, C. Djurberg, F. A. Khan, P. Nordblad, and P. Svedlindh, *Phys. Rev. Lett.* **75**, 4138 (1995); and references therein.
 - ²W. Luo, S. R. Nagel, T. F. Rosenbaum, and R. E. Rosensweig, *Phys. Rev. Lett.* **67**, 2721 (1991).
 - ³C. Djurberg, P. Svedlindh, P. Nordblad, M. F. Hansen, F. Bodker, and S. Morup, *Phys. Rev. Lett.* **79**, 5154 (1997).
 - ⁴T. Jonsson, P. Svedlindh, and M. F. Hansen, *Phys. Rev. Lett.* **81**, 3976 (1998); and references therein.
 - ⁵H. Mamiya, I. Nakatani, and T. Furubayashi, *Phys. Rev. Lett.* **80**, 177 (1998).
 - ⁶J. L. Dormann, D. Fiorani, R. Cherkaoui, E. Tronc, F. Lucari, F. D'Orazio, L. Spinu, M. Noguès, H. Kachkachi, and J. P. Jolivet, *J. Magn. Magn. Mater.* **203**, 23 (1999).
 - ⁷H. Mamiya, I. Nakatani, and T. Furubayashi, *Phys. Rev. Lett.* **82**, 4332 (1999).
 - ⁸J. O. Andersson, C. Djurberg, T. Jonsson, P. Svedlindh, and P. Nordblad, *Phys. Rev. B* **56**, 13983 (1997).
 - ⁹S. Mørup, *Europhys. Lett.* **28**, 671 (1994).
 - ¹⁰P. Jönsson, M. F. Hansen, P. Svedlindh, and P. Nordblad, *Physica B* **284**, 1754 (2000).
 - ¹¹P. Jonsson, M. F. Hansen, and P. Nordblad, *Phys. Rev. B* **61**, 1261 (2000).
 - ¹²Y. Sun, M. B. Salamon, K. Garnier, and R. S. Averback, *Phys. Rev. Lett.* **91**, 167206 (2003), and references therein.
 - ¹³L. Néel, *Ann. Geophys. (C.N.R.S.)* **5**, 99 (1949); W. F. Brown, Jr., *Phys. Rev.* **130**, 1677 (1963).
 - ¹⁴R. K. Zheng, H. Gu, and X. X. Zhang, *Phys. Rev. Lett.* **93**, 139702 (2004); R. K. Zheng, H. Gu, B. Xu, and X. X. Zhang, *Phys. Rev. B* **72**, 014416 (2005).
 - ¹⁵X. X. Zhang, J. M. Hernandez, J. Tejada, and R. F. Ziolo, *Phys. Rev. B* **54**, 4101 (1996); R. K. Zheng, H. W. Gu, B. Xu, and X. X. Zhang, *J. Phys.: Condens. Matter* **18**, 5905 (2006).
 - ¹⁶J. L. Dormann, L. Bessais, and D. Fiorani, *J. Phys. C* **21**, 2015 (1988).
 - ¹⁷F. Luis, F. Petroff, J. M. Torres, L. M. Garcia, J. Bartolome, J. Carrey, and A. Vaures, *Phys. Rev. Lett.* **88**, 217205 (2002).
 - ¹⁸X. X. Zhang, G. H. Wen, G. Xiao, and S. H. Sun, *J. Magn. Magn. Mater.* **261**, 21 (2003), and references therein.
 - ¹⁹J. L. Dormann, D. Fiorani, and E. Tronc, *Adv. Chem. Phys.* **98**, 283 (1997); D. Fiorani, J. Tholence, and J. L. Dormann, *J. Phys. C* **19**, 5495 (1986).
 - ²⁰J. Garcia-Otero, M. Porto, J. Rivas, and A. Bunde, *Phys. Rev. Lett.* **84**, 167 (2000).
 - ²¹S. Mørup and E. Tronc, *Phys. Rev. Lett.* **72**, 3278 (1994).
 - ²²R. H. Kodama, A. E. Berkowitz, E. J. McNiff, Jr., and S. Foner, *Phys. Rev. Lett.* **77**, 394 (1996).
 - ²³B. Martinez, X. Obradors, L. Balcells, A. Rouanet, and C. Monty, *Phys. Rev. Lett.* **80**, 181 (1998).
 - ²⁴S. Sahoo, O. Petracic, W. Kleemann, P. Nordblad, S. Cardoso, and P. P. Freitas, *Phys. Rev. B* **67**, 214422 (2003).
 - ²⁵K. Jonason, E. Vincent, J. Hammann, J.-P. Bouchaud, and P. Nordblad, *Phys. Rev. Lett.* **81**, 3243 (1998).
 - ²⁶V. Dupuis, E. Vincent, J.-P. Bouchaud, J. Hammann, A. Ito, and H. A. Katori, *Phys. Rev. B* **64**, 174204 (2001).
 - ²⁷E. Vincent, cond-mat/0603583, and references therein (unpublished).
 - ²⁸T. Hihara, K. Sumiyama, H. Onodera, K. Wakoh, and K. Suzuki, *J. Phys. Soc. Jpn.* **66**, 1785 (1997), and references therein.
 - ²⁹J. R. Childress and C. L. Chien, *Phys. Rev. B* **43**, 8089 (1991).
 - ³⁰J. A. De Toro, J. P. Andres, J. A. Gonzalez, J. P. Goff, A. J. Barbero, and J. M. Riveiro, *Phys. Rev. B* **70**, 224412 (2004).
 - ³¹J. Q. Xiao, J. S. Jiang, and C. L. Chien, *Phys. Rev. B* **46**, 9266 (1992).
 - ³²A. López, F. J. Lázaro, M. Artigas, and A. Larrea, *Phys. Rev. B* **66**, 174413 (2002).
 - ³³C. S. Barrett and T. B. Massalski, *Structure of Metals*, 3rd ed. (McGraw-Hill, New York, 1966), p. 357.
 - ³⁴P. Allia, M. Coisson, M. Knobel, P. Tiberto, and F. Vinai, *Phys. Rev. B* **60**, 12207 (1999).
 - ³⁵J. A. Mydosh, *Spin Glasses: An Experimental Introduction* (Taylor & Francis, London, 1993).
 - ³⁶R. W. Chantrel and E. P. Wohlfarth, *J. Magn. Magn. Mater.* **40**, 1 (1983).
 - ³⁷F. Lefloch, J. Hammann, M. Ocio, and E. Vincent, *Europhys. Lett.* **18**, 647 (1992).
 - ³⁸E. Vincent, J. P. Bouchaud, J. Hammann, and F. Lefloch, *Philos. Mag. B* **71**, 489 (1995).
 - ³⁹D. S. Fisher and D. A. Huse, *Phys. Rev. B* **38**, 373 (1988); **38**, 386 (1988).
 - ⁴⁰G. J. M. Koper and H. J. Hilhorst, *J. Phys. (Paris)* **49**, 429 (1988).
 - ⁴¹R. Mathieu, P. E. Jonsson, P. Nordblad, H. A. Katori, and A. Ito, *Phys. Rev. B* **65**, 012411 (2001).
 - ⁴²H. Sang, S. Y. Zhang, H. Chen, G. Ni, J. M. Hong, X. N. Zhao, Z. S. Jiang, and Y. W. Du, *Appl. Phys. Lett.* **67**, 2017 (1995); H. Sang, N. Xu, J. H. Du, G. Ni, S. Y. Zhang, and Y. W. Du, *Phys. Rev. B* **53**, 15023 (1996).
 - ⁴³J. A. De Toro, M. A. Lopez de la Torre, J. M. Riveiro, A. Beesley, J. P. Goff, and M. F. Thomas, *Phys. Rev. B* **69**, 224407 (2004).
 - ⁴⁴D. Altbir, J. d'Albuquerque e Castro, and P. Vargas, *Phys. Rev. B* **54**, R6823 (1996).
 - ⁴⁵O. Petracic, X. Chen, S. Bedanta, W. Kleemann, S. Sahoo, S. Cardoso, and P. P. Freitas, *J. Magn. Magn. Mater.* **300**, 192 (2006), and references therein.
 - ⁴⁶B. Zhang, J. Du, and X. X. Zhang (unpublished).